JOURNAL OF MATERIALS SCIENCE 31 (1996) 5701–5708

Characteristics of aerosol-synthesized AlN particles

AN-JAE CHANG, SHI-WOO RHEE*, SUNGGI BAIK
*Department of Materials Science and Engineering, and * Laboratory for Advanced Materials Processing, Department of Chemical Engineering, Pohang University of Science and Technology, Pohang 790-784, Korea*

Particulate characteristics were investigated for AlN synthesized by a thermochemical reaction of aluminium aerosol with ammonia gas. The product powders had a decreasing specific surface area between 15.7 and 36.7 $m^2 g^{-1}$, with increasing reaction temperature from 1100–1500 °C, and the powders with large surface area were strongly hygroscopic. Although the powders were severely aggregated and had a small amount of unreacted aluminium, light milling and post heat treatment made them ultrafine and completely converted. When sintered with 0.5% yttrium at 1900 °C, full densification and high thermal conductivity of about 130 $W m^{-1} K^{-1}$ were obtained.

1. Introduction

Aluminium nitride (AlN) is projected to be the prime material for making IC substrates and packages [1]. In addition, its high thermal conductivity, high dielectric strength, high mechanical strength, and a thermal expansion close to silicon, make this material ideal for miniaturization, high-power chips, and multichip modules [2]. However, the application of AlN is limited because of the higher price of raw material compared with alumina. Although the conventional direct nitridation synthesis process is one of the large-scale methods for producing commercial AlN powders, it is still difficult to make fine and fully converted powders without coagulation of metallic powders during the process [3].

To develop an improved process, several researchers have attempted the direct nitridation of dispersive metallic powder [4–6]. This approach was successful for the nitridation of aluminium aerosol in a nitrogen gas stream, and, in particular, fine powders below 0.2 μm were synthesized within a very short reaction time. It has also been reported that the control of the conversion or wall-deposition of the product powder was accomplished efficiently by varying the process conditions [7, 8]. Ammonia addition lowered the nitridation temperature successfully [9] and this is regarded to be due to the reactive nitrogen-containing radicals induced by the thermal decomposition of ammonia participating in the reaction [10, 11]. The degree of nitridation would depend strongly on various process parameters related to the ammonia dissociation.

In this paper, we report the influence of ammonia and reaction temperature on the characteristics of AlN powders synthesized from aluminium aerosol. Physical and chemical analyses were performed on the product powders and microstructural analysis with mercury porosimetry was also carried out to examine the morphological changes.

2. Experimental procedure

2.1. Powder preparation and characterization

Five kinds of AlN powder were synthesized by direct nitridation of aluminium aerosol. Reaction temperatures were between 1100 and 1500 °C, and the NH_3/Al mole ratio was 24.1. The synthesis procedure was described in more detail elsewhere [12]. All the post-treatment steps for product powders were carried out under an inert and dehumidified atmosphere to avoid further oxidation or hydrolysis during the processing.

Specific surface areas of the powders were measured by a five-point BET (AutoSorb-2100E, Micrometrics, USA). Oxygen and nitrogen contents were also measured using an oxygen/nitrogen determinator (TC-136, LECO, USA) with nickel and tin as fluxes at 1900 °C. Typical impurities in AlN powder, e.g. silicon, iron, and carbon, were measured using an inductively coupled plasma emission spectrometer (ICP; PS-4, Baird, USA) and carbon/sulfur determinator (CS-044, LECO, USA) with iron, copper and tungsten fluxes at 1800 °C, respectively. A scanning electron microscope (JSM 5400, Jeol, Japan) and a transmission electron microscope (JEM 4000FX, Jeol, Japan) were used to analyse the powder morphologies. Other particulate characteristics, such as particle size, structure, hygroscopic behaviour, and unreacted aluminium content, were also analysed using a particle-size analyser, a high-pressure mercury porosimeter (Autopore II 9220, Micrometrics, USA) a Fourier

0022–2461

transform-infrared (FT–IR) spectrometer (1725X, Perkin-Elmer, UK) and a thermogravimetric analyser (TGA 92, Setaram, France).

2.2. Sintering and evaluation

Yttria (Y_2O_3) was added in the form of yttrium nitrate ($Y(NO_3)_3 \cdot 5H_2O$) as a sintering additive. The AlN powder and additive were mixed in isopropyl alcohol. A commercially available AlN powder (Toyalnite-F, Toyo Aluminium, Japan; purity 99.9%, specific surface area 3.4 $m^2 g^{-1}$, oxygen content 1.76 wt %) was treated under the same conditions for comparison with the synthesized powder. After being dried and isostatically pressed into cylindrical compacts at 145 MPa, they were sintered in a BN-coated alumina saggar and heated with a graphite furnace in flowing nitrogen gas. The heating rate was 15 °C min^{-1} and the sintering temperatures were 1700 or 1900 °C, respectively. The holding time at each temperature was 1 h. The densities of the sintered specimens were measured by the displacement method using water. Scanning electron microscopy was used to observe the microstructural evolution after sintering. Thermal conductivity and electrical resistivity were also measured for the densified specimens by the laser flash method (TC 7000, Shinku-Riko, Japan) and pico-ammeter (PA meter 4140B, Hewlett Packard, USA), respectively.

3. Results and discussion

3.1. General characteristics of product powders

The changes in characteristics of the product powders obtained at different temperatures between 900 and 1500 °C are shown in Fig. 1. The conversion of aluminium of AlN was saturated at approximately 0.9 above 1100 °C while specific surface areas of the powders decreased from 36.7 $m^2 g^{-1}$ to 15.7 $m^2 g^{-1}$ with elevating temperature. A higher mole ratio of NH_3/Al, on the other hand, did not affect them significantly. Wall-deposited powders after 3 h reaction at 1300 °C showed a higher conversion of 0.95 and lower surface area of 10.7 $m^2 g^{-1}$.

The microstructures of the powders formed at 900, 1100, 1300 and 1500 °C are shown in Fig. 2. The particle shape and surface morphology changed remarkably with increasing temperature. The increase in surface area up to 1100 °C resulted from the increasing nucleation sites with increasing conversion, while the decrease above 1100 °C presumably resulted from the coalescence of crystallites on the particle surface with increasing temperature. In the powders formed at 1500 °C (Fig. 2d), melt-extraction from the particle core was obviously observed. Particle-size analysis also showed an appreciable increase in median diameters with increasing temperatures: 9.8, 14.7, 15.8 and 15.9 μm for Fig. 2a, b, c and d, respectively. Porosimetric analysis for powders formed at 900–1500 °C indicated the hollow structure of particles covered with a porous product layer. In Fig. 3, plots of the intruded volume of mercury versus pore

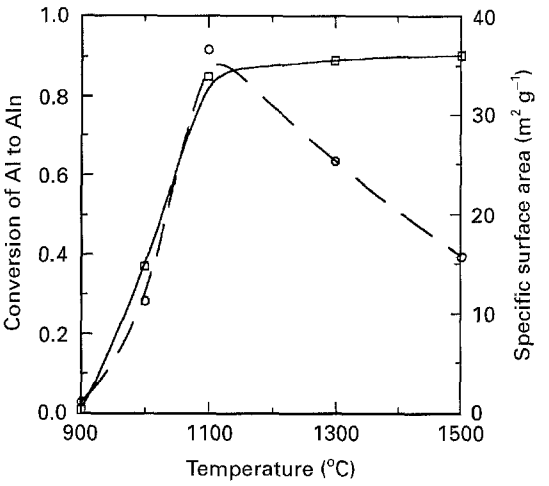

Figure 1 Effect of reactor temperature on (–□–) aluminium conversion and (--○--) specific surface area of product powders at an NH_3/Al mole ratio of 24.1.

radius are shown for each powder. Pressure was applied to force mercury into the voids and pores. Depending on the particle size, size distribution, shape, and packing geometry, inter-particle voids exist of various dimensions and shapes, which are progressively filled as the pressure increases [13]. Total intrusion volumes of mercury were 0.61, 0.83, 1.25 and 1.82 ml g^{-1}, respectively. The initial positive slopes in the intrusion curve were due to the penetration of mercury into the inter-particle voids of powders. As the pressure increases, the intrusion began into a new range of cavities of about 5 μm radius in the powder. The increase in cumulative pore volume from (a) to (d) presumably resulted from the enlarging inter-particle or intra-particle voids of product powders formed at elevating reaction temperature. The slightly positive slopes below 1 μm pore size resulted from continued filling of the submicrometre pores in the nitrided layer of particles. This was due to the porous structure of nitrided particles, especially hollow particle structure for powders synthesized at higher temperature. Such results strongly support the previously proposed nitridation mechanisms, the gas-penetration at low temperatures and the melt-extraction at high temperatures above 1200 °C [12].

As-produced powders, even though the average particle size was about 10 μm, could be easily crushed by light milling to a very fine size as shown in Fig. 4. During the powder processing in an ambient atmosphere, however, the hydrolysis of the synthesized powder proceeded slowly depending on the powder surface area. Fig. 5 shows the increase in weight with time when the as-produced powders were exposed to 90% relative humidity at 30 °C. The powder with higher surface area (36.7 $m^2 g^{-1}$) exhibited higher increase in weight than that with lower surface area (15.7 $m^2 g^{-1}$). This is consistent with the report that the rates of hydrolysis and oxidation of AlN powder depend strongly on environmental conditions as well as powder surface area [14]. The hydrolysis of powder could be monitored by FT–IR spectroscopy which provides chemical information resulting from the assignment of absorption bands to distinct chemical

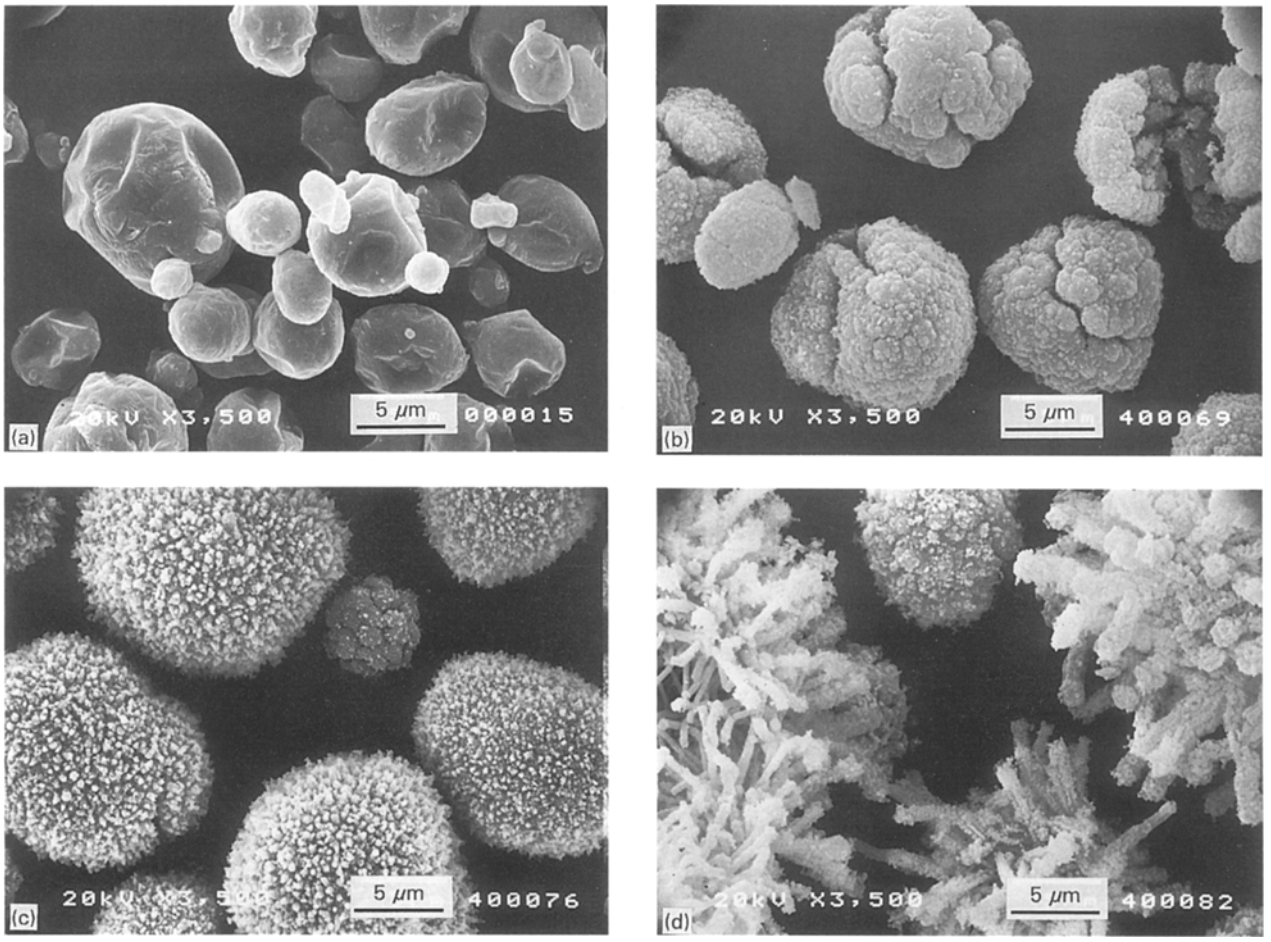

Figure 2 Scanning electron micrographs of product powders formed at a reactor temperature of (a) 900 °C, (b) 1100 °C, (c) 1300 °C, and (d) 1500 °C.

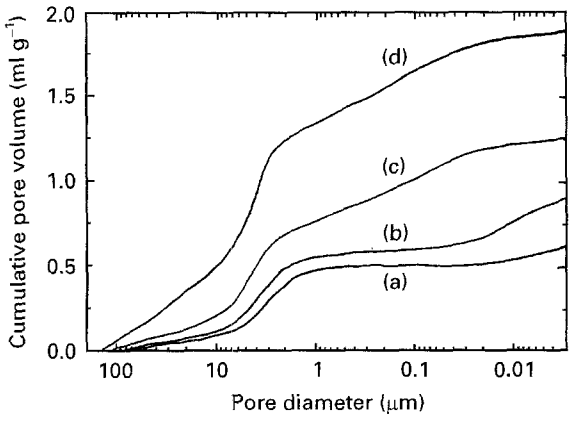

Figure 3 Cumulative pore volume versus pore diameter plot for powders formed at temperatures of (a) 900 °C, (b) 1100 °C, (c) 1300 °C, and (d) 1500 °C.

species. Fig. 6 shows three infrared spectra obtained for powders which were as-produced, exposed and hydrolysed, and subsequently thermally-treated. While absorption due to AlN was minimal for the as-produced powder, strong sharp absorption bands were observed in the regions 1200–1400 and 3200–3600 cm^{-1} for the exposed powder. After the heat treatment, however, the absorption bands have disappeared, replaced by the stronger Al–N band of 600–800 cm^{-1}.

3.2. Effects of post-treatment on powder characteristics

As explained in the previous section, complete conversion to AlN is difficult to reach with this single-reaction process, which seems to have resulted from the nitride coating layer inhibiting the diffusion of reactant gas to unreacted aluminium in the core. An intermediate milling step was generally required in the direct nitridation method in order to achieve complete conversion by post-reaction heat treatment after exposing unreacted aluminium [8]. Fig. 7 shows weight change as a function of temperature in a nitrogen atmosphere for (a) as-produced at 1300 °C (13-T0) and (b) subsequently dry-milled powder (13-T1). There was no weight change for as-produced powders and it seemed that unreacted aluminium in the core did not change in the nitrogen atmosphere. On the other hand, dry-milled powders showed a weight decrease and it seemed that unreacted aluminium within the core of particles was exposed by the milling step and evaporated without being nitrided. The 13-T1 powder was placed into a quartz crucible and further nitrided at 1100 °C for 3 h to a fine white powder. The results are summarized in Table I. The post heat-treated powder (13-T2) was completely converted to AlN after the reaction step. The theoretical nitrogen content in pure AlN is 34.2 wt %. The amount of impurities, including oxygen, and the specific surface area, changed little after the post-treatment.

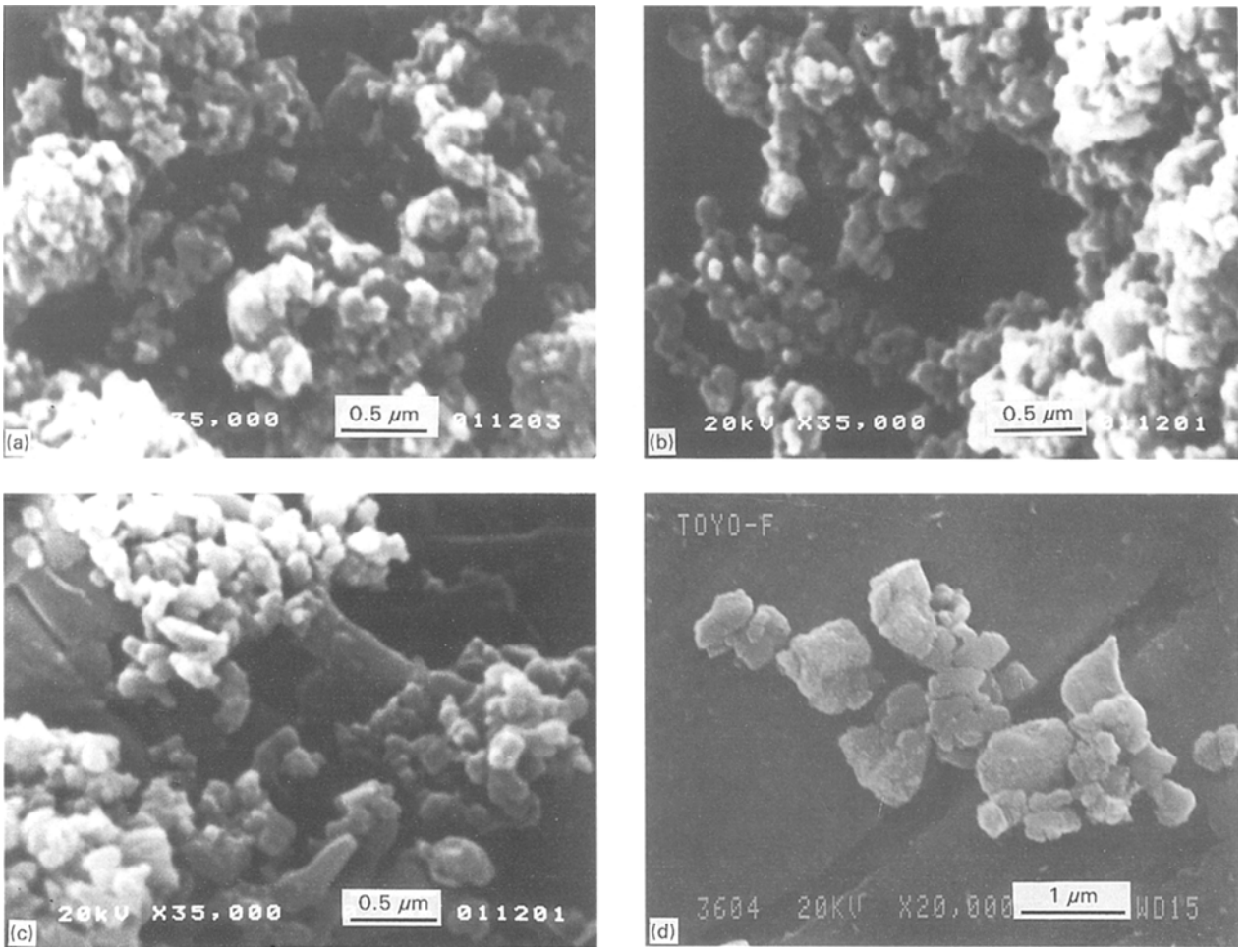

Figure 4 Scanning electron micrographs of dry-milled powders which were formed at reactor temperatures of (a) 1100 °C, (b) 1300 °C, and (c) 1500 °C; (d) commercial AlN powder manufactured by the direct nitridation method.

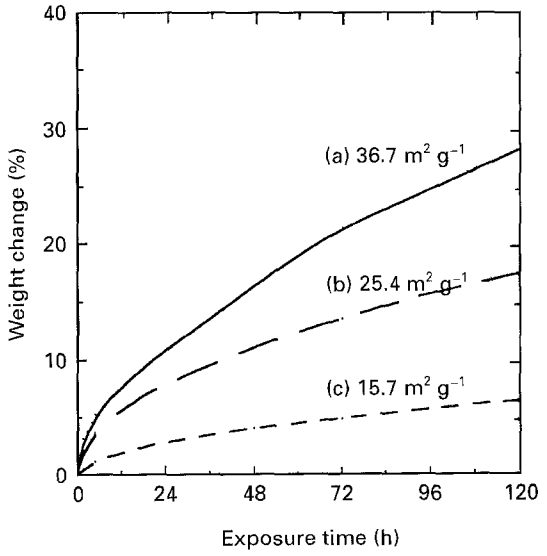

Figure 5 Weight gains of product powders as a function of exposure time under 90% relative humidity at 30 °C; samples were formed at (a) 1100 °C, (b) 1300 °C, and (c) 1500 °C.

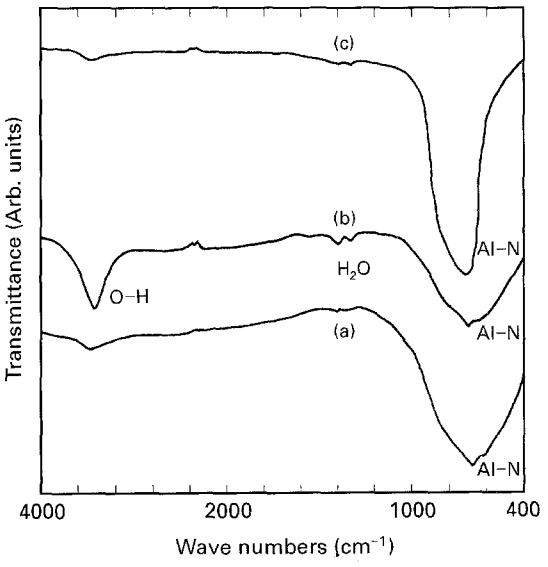

Figure 6 Fourier transform–infrared spectroscopic analysis of product powders which are (a) as-produced (13-T0), (b) hydrolysed under humid conditions, and (c) subsequently thermally treated.

Transmission electron micrographs in Fig. 8 show the ultrafine AlN crystallites of the samples, which were formed at 1100, 1300, 1500 °C and subsequently dry-milled. As shown in Fig. 8a, the powder formed at 1100 °C was severely aggregated and consisted of ultrafine crystallites. Its average size was determined to be 0.025 μm from the following equation [15]

$$d_{BET} = 3/(S\rho_{th}) \quad (1)$$

where d_{BET} is the BET-equivalent particle size (μm), S is the specific surface area ($m^2 g^{-1}$), and ρ_{th} is the

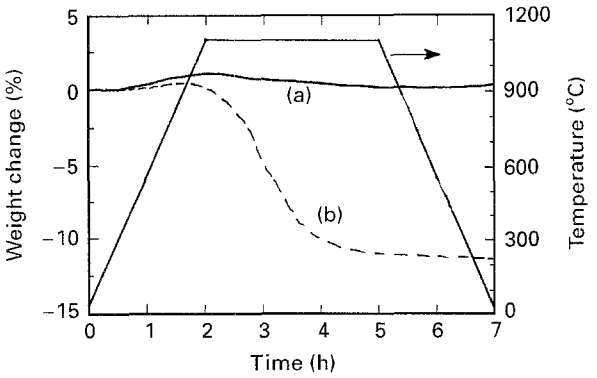

Figure 7 Thermogravimetric analysis in a nitrogen atmosphere for (a) as-produced (13-T0) and (b) subsequently dry-milled (13-T1) powders.

TABLE I Effects of post-treatment on the characteristics of the product powder

Sample powder	Nitrogen (wt %)	Oxygen (wt %)	Specific surface area ($m^2 g^{-1}$)
As-produced at 1300°C (13-T0)[a]	30.4	1.43	25.4
Dry-milled and heat-treated (13-T2)	33.0	2.85	25.1

[a] Impurities: 0.077% Si, 0.10% Fe, 0.032% C.

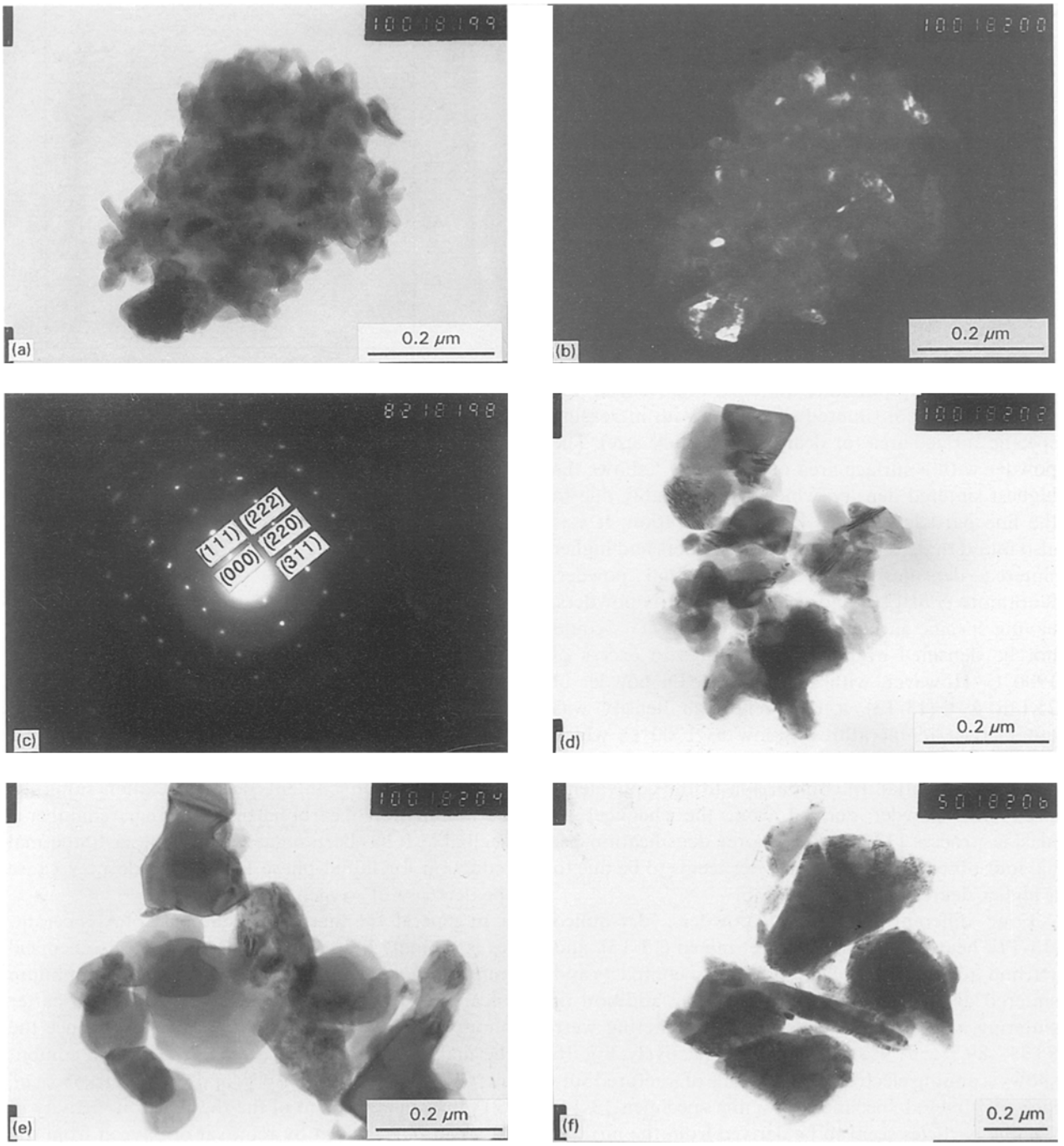

Figure 8 Transmission electron micrographs of dry-milled powders for (a) 1100 °C-produced powder; (b, c) dark-field image and selected-area diffraction pattern for the white phase of (a); (d–f) are for 1300 °C, 1500 °C-produced and commercially available directly nitrided AlN powder, respectively.

theoretical density of a solid particle ($g\,cm^{-3}$). Dark-field TEM analyses shows that AlN aggregates contain a small amount of unreacted aluminium. Fig. 8b shows the dark-field image, where the metallic aluminium appears white in colour. Its selected area diffraction pattern shown in Fig. 8c confirms that the white areas represent the unreacted aluminium. On the other hand, the powder synthesized at 1300 °C (Fig. 8d) has a much larger mean size and shows no evidence of agglomerate formation. The mean particle size ranges between 0.02 and 0.1 μm. The particles formed at 1500 °C (Fig. 8e) are large, uniform, and loosely agglomerated. Its BET-equivalent size is 0.06 μm. Fig. 8f shows the commercial AlN powder synthesized by direct nitridation, which has a much larger particle size and wide size distribution with various particle shapes.

For the AlN powders which were formed at different temperatures, the characteristics after the post-treatment are listed in Table II. The samples 11-T2, 13-T2, and 15-T2, were dry-milled and subsequently thermally treated powders which were obtained at reaction temperatures of 1100, 1300, and 1500 °C, respectively. Except for the particle size, the differences between the synthesized powders and commercial powder (RF-T2) are insignificant.

3.3. Sintering characteristics

Five kinds of AlN powder having different specific surface areas (11-T3 to 15-T3) were sintered at 1700 and 1900 °C without sintering aids. Fig. 9 shows the relative density of sintered specimens with increasing specific surface area (or decreasing particle size). The powder with a surface area of 25.1 $m^2\,g^{-1}$ shows the highest sintered density, which is presumably due to the fine particle size and less agglomeration. It was also found that all the synthesized powders had higher sintered densities than the commercial powder. Kuramoto *et al.* [16] had reported that AlN powders, having specific surface areas around 3 $m^2\,g^{-1}$, could not be densified even at temperatures in excess of 1900 °C. However, with synthesized AlN powder of 25.1 $m^2\,g^{-1}$ (13-T3), a relatively high density was obtained at temperatures as low as 1700 °C, which indicates that this material possesses favourable densification potential. In comparison to the equivalent-sized AlN powder derived from the chemical or plasma process [17, 18], the poorer densification behaviour observed with our powder seems to be due to a higher degree of agglomeration.

Four different batches of powders, dry-milled (13-T1), heat-treated (13-T2), wet-mixed (13-T3), and yttrium-added (13-T4), were pressed to compacts and sintered at 1900 °C for 1 h without the addition of sintering aids. Relative densities after sintering were 85.9%, 89.5%, 91.9%, and 99.3%, respectively. Fig. 10 shows scanning electron micrographs of fractured surfaces of sintered specimens. For the specimen 13-T1, the fine particles seem to be derived from the nitridation of unreacted metallic aluminium during sintering. For the specimens from post-treated powder, large pores disappear and neck growth occurs. The presence of a glassy phase was not observed for those specimens. For specimen 13-T4, pore-free microstructure with uniform grain size was obtained, as shown in Fig. 10d.

TABLE II Chemical and physical characteristics of the synthesized AlN powders[a]

Sample (Temp., °C)	N (wt %)	O (wt %)	Specific surface area ($m^2\,g^{-1}$)	$\bar{d}^{b}_{BET}$ (μm)
11-T2 (1100)	32.5	3.79	36.7	0.03
13-T2[c] (1300)	33.0	2.85	25.1	0.04
15-T2 (1500)	32.2	2.33	15.7	0.06
RF-T2[d]	32.9	2.59	3.4	0.27

[a] After heat treatment.
[b] BET-equivalent size determined by Equation 1.
[c] Impurities: 0.062% Si, 0.10% Fe, 0.044% C.
[d] Heat-treated commercial AlN powder.

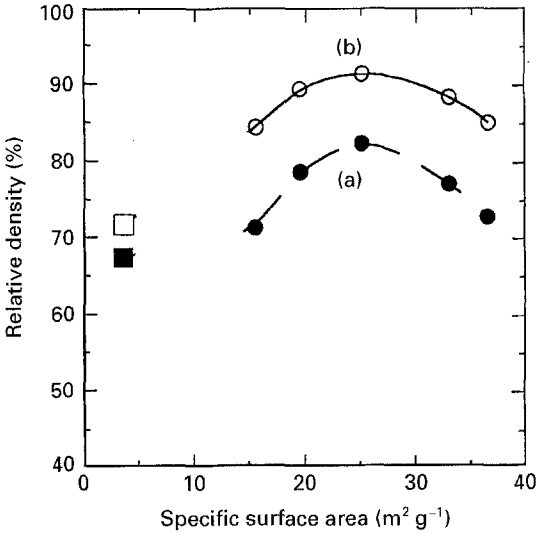

Figure 9 Effects of particle size on densification of synthesized AlN powders without sintering aids; samples were sintered at (●) 1700°C and (○) 1900 °C for 1 h. (■, □) Commercial powder, sintered at (■) 1700 °C and (□) 1900°C.

Table III shows the properties of the fully densified AlN specimens at 2000 °C. The specimen shows high electrical resistivity above $10^{12}\,\Omega$ cm and high thermal conductivity of 130 $W\,m^{-1}\,K^{-1}$. It is also noticeable that the oxygen content decreased after sintering. Contamination of carbon from the furnace chamber is negligible. It has been suggested that the carbothermal reduction for liquid-phase forming oxide may cause the decrease of oxygen content [19].

In general, the thermal conductivity of AlN ceramics is strongly influenced by density and its chemical purity. Slack *et al.* [20] proposed that aluminium vacancies created by oxygen impurities scatter phonons mostly from the AlN lattice, and hence the thermal conductivity decreases as the oxygen content increases. It has been also proposed by Virkar *et al.* [21] that enhancement of the thermal conductivity of AlN can be achieved by removal of oxygen from the lattice of AlN. High thermal conductivity of the specimen suggests that a smaller amount of oxygen is dissolved in AlN grains.

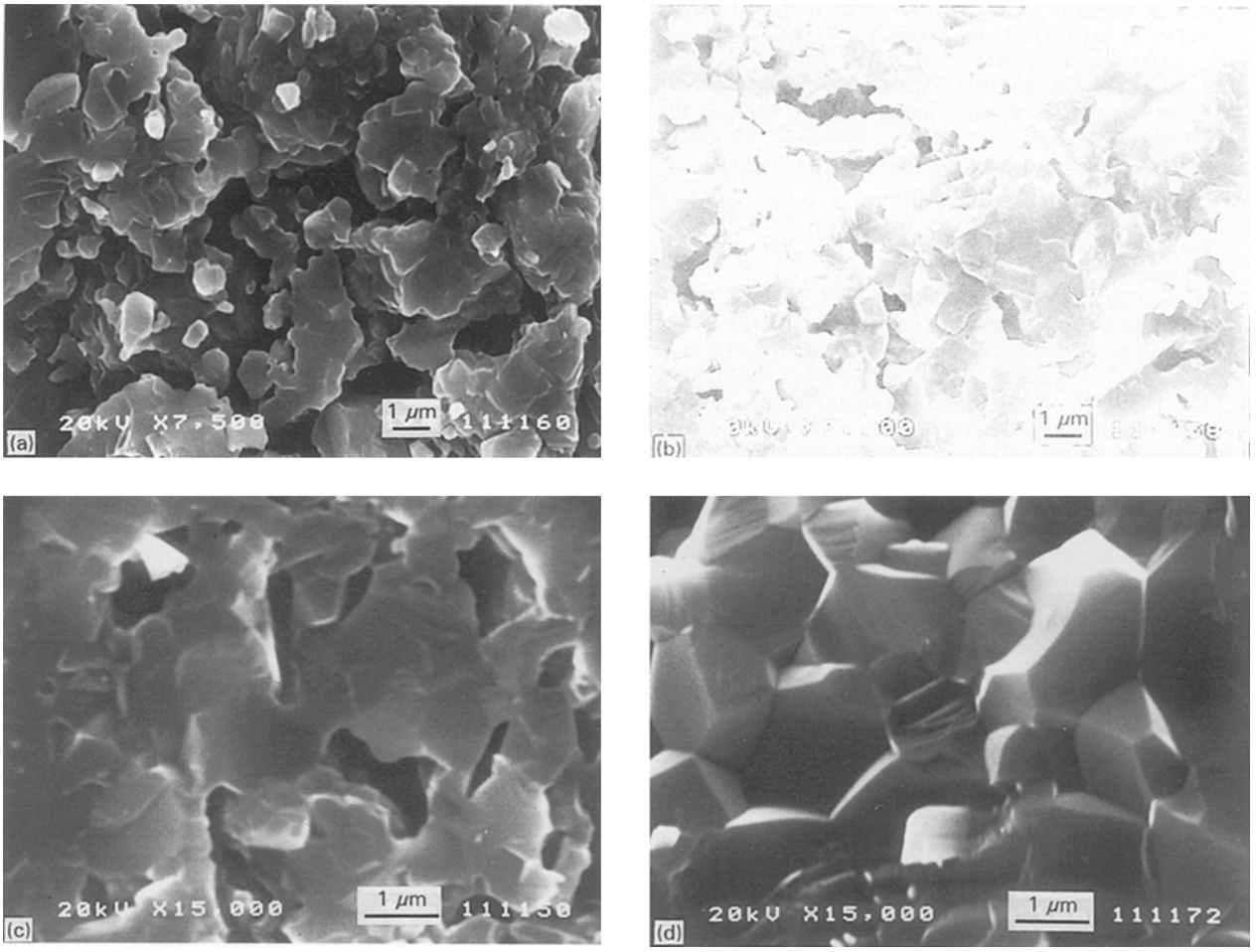

Figure 10 Scanning electron micrographs of the fractured surface of sintered samples (at 1900 °C for 1 h); each sample was from (a) as-produced and subsequently dry-milled (13-T1), (b) heat-treated (13-T2), (c) wet-mixed (13-T3), and (d) yttrium-added (13-T4) powders.

TABLE III Properties of AlN specimen[a] sintered with 0.5% Y-addition

Thermal conductivity (R.T.) ($W m^{-1} K^{-1}$)	129.6
Electrical resistivity (R.T.) (Ω cm)	$> 10^{12}$
True density ($g cm^{-3}$)	3.27
Oxygen content (wt %)	1.51

[a] Sintered specimen from the 13-T2 powder (at 1900 °C for 1 h).

4. Conclusions

AlN powders synthesized by direct nitridation of aluminium aerosol were characterized and the results are summarized as follows.

1. The synthesized powders consisted of very fine particles below 0.1 μm and had a small amount of unreacted aluminium encapsulated in the nitride layer.

2. In an ambient atmosphere, the powders showed a hygroscopic nature due to their high specific surface areas.

3. Unreacted aluminium and particle agglomeration prevented the powder compacts from becoming fully densified even though the finer powder was favourable for the densitification.

4. After the post-treatment step, the sintering temperature for the synthesized powder was lowered to a larger extent than that of commercial AlN powder.

5. For the fully densified specimen at 1900 °C with 0.5 at % yttrium addition, the thermal conductivity was 130 $W m^{-1} K^{-1}$.

Acknowledgements

The authors would like to thank Mr Dong-sik Kim, researcher in POSTECH and Dr Yong-ha Kim, Researcher in Research Institute of Industrial Science and Technology (RIST), for their analytical support and encouragement.

References

1. D. G. WIRTH, in "Engineered Materials Handbook", Vol. 4, edited by S. J. Schneider Jr (ASM International, Materials Park, OH, 1991) p. 1107.
2. W. WERDECKER and F. ALDINGER, *IEEE Trans. Compos. Hybrids, Manuf. Technol. CHMT-7* **4** (1984) 399.
3. T. J. MROZ Jr, *Am. Ceram. Soc. Bull.* **72** (1993) 78.
4. S. MATSUO, N. HOTTA and Y. NISHWAKI, *Yogyo-Kyokai-Shi* **83** (1975) 490.
5. N. HOTTA, I. KIMURA, A. TSUKUNO, N. SAITO and S. MATSUO, *ibid.* **95** (1987) 274.
6. K. TSUKAMOTO, E. ISOYAMA and N. HOTTA, Jpn. Pat. 63-195102 (1988).
7. A. W. WEIMER, G. A. COCHRAN, G. A. EISMAN, J. P. HENLEY, T. A. GUITON, A. K. KNUDSEN and N. R. NICHOLAS, *Aerosol. Sci. Technol.* **19** (1993) 491.
8. A. W. WEIMER, G. A. COCHRAN, G. A. EISMAN, J. P. HENLEY, B. D. HOOK, L. K. MILLS, T. A. GUITON,

A. K. KNUDSEN, N. R. NICHOLAS, J. E. VOLMERING and W. G. MOORE, *J. Am. Ceram. Soc.* **77** (1994) 3.
9. I. KIMURA, K. ICHIYA, M. ISHII and N. HOTTA, *J. Mater. Sci. Lett.* **8** (1989) 303.
10. A. CHANG, S. RHEE and S. BAIK, *J. Am. Ceram. Soc.* **178** (1995) 33.
11. *Idem, Proc. Kor. Jpn. Seminar New Ceram.* **11** (1994) 48.
12. *Idem, J. Mater. Sci.* **30** (1995) 1180.
13. S. LOWELL and J. SHIELDS, in "Powder Surface Area and Porosity", 2nd Edn edited by B. Scarlett (Chapman and Hall, London, 1984) p. 97.
14. M. S. PAQUETTE, J. L. BOARD, C. N. HANEY, A. K. KNUDSEN, D. W. SUSNITZKY, P. R. RUDOLF, D. R. BEAMAN, R. A. NEWMAN and S. W. FROELICHER, in "Ceramic Transactions", Vol. 12, edited by G. L. Messing, S.-I. Hirano and H. Hausner (American Ceramic Society, Westerville, OH, 1990) p. 855.
15. S. LOWELL and J. SHIELDS, in "Powder Surface Area and Porosity", 2nd edn edited by B. Scarlett (Chapman and Hall, London, 1984) p. 3.
16. N. KURAMOTO, H. TANIGUCHI and I. ASO, *Adv. Ceram.* **26** (1989) 107.
17. N. HASHIMOTO, H. YODEN and S. DEKI, *J. Am. Ceram. Soc.* **75** (1992) 2098.
18. U. AIKAWA, K. BABA and N. SHOUHATA, in "Micro-Electronics Symposium" (1989).
19. M. YOKOI, T. KANEMURA, M. KUMAGAI, T. NAKANO, T. FUNAHASHI and Y. YOSHII, *Kawasaki Steel Giho* **21** (1989) 287.
20. G. A. SLACK, R. A. TANZILLI, R. O. POHL and J. W. VANDERSANDE, *J. Phys. Chem. Solids* **48** (1987) 641.
21. A. V. VIRKAR, T. B. JACKSON and R. A. CUTLER, *J. Am. Ceram. Soc.* **72** (1989) 2031.

Received 20 February
and accepted 1 December 1995